Role of spin orbit interaction potential in two nucleon transfer reactions

Rajni[1], Ishita Sharma[1], Deepika Jain[2], and Manoj K Sharma[1]
[1]*School of Physics and Materials Science, Thapar University, Patiala, India. and*
[2]*Department of Physics, Mata Gujri College, Fatehgarh Sahib, India.*

Introduction

Fusion of two nuclei depends on the barrier characteristics of interaction potential used in form of Coulomb, centrifugal, and nuclear proximity potentials. The short range nuclear potential strongly depends on the the nuclear surface properties and readjustment of composite nuclear system, resulting in potential pocket. Nuclear surface properties can be described by variety of interaction potentials available in the literature. In this work, the Skyrme energy density formalism (SEDF) [1] based on semi-classical extended Thomas fermi approach is used to address the nuclear proximity potential. The nucleus-nucleus potential calculated within the framework of SEDF provides an opportunity to treat spin-orbit dependent V_J and spin-orbit independent V_P part of interaction potential separately.

In the present work, an attempt is made to study the significance of deformations on spin-orbit density dependent potential in reference to two nucleon transfer reactions forming the same compound system (^{72}Se*). The calculations are done for both spherical as well as deformed choice of fragments. It is observed that, for spherical choice of interaction, the barrier height and barrier position remains unaffected for all the five reactions (^{23}Na+^{49}V,^{25}Mg+^{47}Ti,^{27}Al+^{45}Sc,^{29}Si+^{43}Ca and ^{31}P+^{41}K) formed using the two nucleon transfer process. On the other hand, the inclusion of deformation and related orientation effects modify the barrier height and position considerably. The fusion cross-sections of ^{72}Se* formed via ^{23}Al+^{45}Sc reaction [2], are estimated using dynamical cluster decay model (DCM) [3] with and without taking contribution of spin-orbit part in total interaction potential. The results show that the contribution of V_J to fusion cross-section is of significant importance.

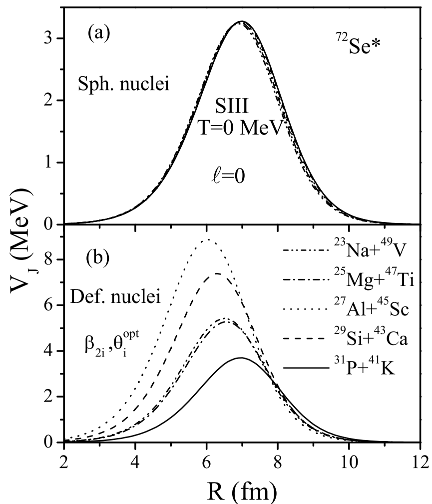

FIG. 1: The spin-orbit interaction potential V_J as a function of R at T=0 for two nucleon transfer products starting with ^{23}Na+^{49}V using SIII force for (a) Spherical nuclei and (b) β_2-deformed nuclei.

Methodology

In dynamical cluster-decay model (DCM) [3] the compound nucleus decay cross-section is calculated by using partial wave analysis in terms of preformation probability (P_0) and barrier penetrability P.

The fragmentation potential used to address preformation probability comprises of binding strength, nuclear potential, Coulomb potential and angular momentum dependent potential. Here we have calculated the nuclear proximity potential by using SEDF approach.

The skyrme energy density formalism

(SEDF), defines the nuclear interaction potential as

$V_N(R)=E(R)-E(\infty)=V_P(R)+V_J(R)$

Where $V_P(R)$ represents the spin saturated part of interaction potential and $V_J(R)$ accounts for the spin dependent interaction.

Calculations and Results

We have calculated the spin-obit density dependent potential for the colliding series of $^{23}Na+^{49}V$, $^{25}Mg+^{47}Ti$, $^{27}Al+^{45}Sc$, $^{29}Si+^{43}Ca$ and $^{31}P+^{41}K$ all giving the same compound system $^{72}Se^*$, by using SIII force within the framework of semi-classical extended Thomas fermi approach (ETF) of the Skyrme density formalism (SEDF). Fig. 1(a) shows that for spherical choice of colliding nuclei, the barrier height (V_{JB}) and barrier position (R_{JB}) remain almost constant with simultaneous addition and stripping of two nucleon in the projectile and target respectively. However, on allowing deformation effects as depicted in Fig. 1(b), the barrier height V_{JB} increases with enhanced magnitude and the barrier position R_{JB} shift towards smaller interaction radius, compared to the one obtained for spherical case. The enhancement in V_{JB} and reduction in R_{JB} is much higher for oblate shape nuclei followed by prolate and spherical nuclei. This observation is in agreement with results of [4], carried out for heavier nuclei with mass A∼156-172. It means that, the different spherical reacting partners forming same compound nucleus, experience the maximum repulsion at about same distance, whereas the deformed nuclei suffer maximum repulsion at different interaction radii. Thus the inclusion of deformations in spin-orbit interaction potential play a significant role to study nuclear interaction potential and consequently affect the fusion cross-sections of different nuclear systems.

Further, we have calculated the fusion cross-sections of $^{23}Al+^{45}Sc$ reaction within the frame work of DCM using deformed choice of decaying fragments. The calculations are done with the inclusion and exclusion of spin-orbit interaction part in the total interaction potential as shown in Table I. It is anticipated from the table that, the spin dependent part of interaction potential contributes significantly towards the fusion cross-sections, which inturn find a decent agreement with available experimental data. Therefore one may conclude that V_J component plays important role in the fusion dynamics of nuclear systems. It would be of further interest to study the relative contribution of spin-orbit part calculated using different sets of Skyrme forces, employed to address the ground as well as exotic states associated with nuclear dynamics.

TABLE I: The fusion cross-sections for $^{72}Se^*$ system, calculated using the DCM with deformed choice of nuclei at different $E_{c.m.}$'s for SIII skyrme force compared with the experimental data [2].

$E_{c.m.}$ (MeV)	Temp. (MeV)	σ^{fusion}_{DCM}(mb) V_P+V_J	V_P	$\sigma_{Expt.}$(mb)
31.74	2.337	2.03×10^{-4}	2.26×10^{-5}	2.76×10^{-4}
32.49	2.357	0.00270	5.23×10^{-4}	0.00245
33.06	2.373	0.0101	2.47×10^{-3}	0.0104
33.67	2.389	0.0418	1.28×10^{-2}	0.0425
34.28	2.406	0.153	5.63×10^{-2}	0.152
34.85	2.421	0.582	0.292	0.574
35.50	2.438	2.06	1.19	2.038
36.46	2.463	8.39	5.47	8.248
37.62	2.493	21.6	15.1	21.932
38.48	2.515	49.6	37.0	48.130
39.41	2.539	64.1	46.7	65.98
40.75	2.572	121	95.9	122.19
42.48	2.615	174	142.0	175.70
44.78	2.671	255	213.0	255.49
47.42	2.733	424	363.0	424.86
50.05	2.794	598	555.0	611.29

References

[1] R. K. Gupta *et al.*, J. Phys. G: Nucl. Part. Phys. **36**, 075104 (2009).

[2] C. L. Jiang *et al.*, Phys. Rev. C **81**, 024611 (2010).

[3] Rajni *et al.*, Phys. Rev. C **90**, 044604 (2014).

[4] D. Jain *et al.*, Eur. Phys. J. A **50**, 155 (2014).